JOURNAL OF SPACECRAFT AND ROCKETS
Vol. 31, No. 3, May–June 1994

Solid Rocket Exhaust in the Stratosphere: Plume Diffusion and Chemical Reactions

M. Richard Denison,* John J. Lamb,† William D. Bjorndahl,‡ Eric Y. Wong,§ and Peter D. Lohn¶
TRW, Inc., Redondo Beach, California 90278

A model has been developed to examine, on a local scale, the reactions of rocket exhaust from solid rocket motors with stratospheric ozone. The effects were examined at two different altitudes. Results of the modeling study indicate that afterburning chemistry of reactive exhaust products can cause local but transient (on the order of several minutes) loss of ozone. The modeling study included potential heterogeneous reactions at aluminum oxide surfaces. Results indicate that these potential heterogeneous reactions do not have a major impact on the local plume chemistry. Homogeneous reactions appear to be of more consequence during the early dispersion of the plume. It has also been found that the rate of plume dispersion has a very significant effect on local ozone loss.

Nomenclature

a = radius of cylinder under consideration
K = apparent eddy diffusion coefficient
l = scale of the plume
N = volume density of species N
N_0 = initial volume density of species N
$\dot{R}_N$ = net rate of production of species N
$R(\tau)$ = Lagrangian correlation function
r = plume radius
t = time
t_L = Lagrangian time scale
$\overline{u'^2}$ = mean square of velocity fluctuation

Introduction

THE possible impact of the exhaust of solid rocket motors (SRMs) on the environment has been studied by the Department of Transportation in the early 1970s as part of the Climatic Impact Assessment Program (CIAP).[1] The results of these studies showed minimal impact on stratospheric ozone by the rocket effluents. Intensive work in the area of atmospheric chemical kinetics since that time has yielded new rate constants for many of the important reactions involving ozone destruction. Also, in the last few years there has been renewed interest in the stratospheric effects of rocket effluents. Several modeling investigations have been carried out recently.[2-5] These studies have come to different conclusions on local ozone depletion in the vicinity of the rocket plume. The study described in this paper addresses the question of local ozone depletion by modeling the chemistry starting in the rocket combuster and nozzle, taking into account afterburning chemistry and dispersion in the hot plume, and then by modeling the chemistry and diffusion in the cool plume.

The major exhaust products from ammonium perchlorate/aluminum SRMs are hydrogen chloride (HCl), aluminum oxide (Al_2O_3), water (H_2O), hydrogen (H_2), carbon monoxide (CO), and carbon dioxide (CO_2).[6] Note that these species are the primary exit plane species; no afterburning in the plume is taken into account. It has been suggested that substantial local reductions in ozone are possible due to reactions of chlorine contained in the HCl.[4] It has also been suggested that aluminum oxide may provide surfaces for heterogeneous reactions or may provide condensation nuclei for stratospheric aerosol particles.[7]

In their report to Congress and subsequent journal article on the impact of rocket launches on stratospheric chemistry, Prather et al.[2,3] noted that the local depletion of ozone near the rocket plume could be significantly different from that calculated by global models that do not resolve such details. They argue that, to have a significant effect on global ozone, the plume must cause measurable perturbations over scales of at least 1000 × 1000 km. They point out that the amount of chlorine injected into the stratosphere from a vehicle such as the Space Shuttle is negligible compared with the ambient chlorine on such a scale. In terms of local ozone depletion, they point out that the flight path of such rocket launches is not vertically aligned and the exhaust gases are expected to spread over 1000 km in a day so that no local hole in column ozone could occur over the launch site. They also contend that local ozone depletion is unlikely because the hydrogen chloride in the exhaust would require some time to be converted into more catalytically active forms. In addition, data from the total ozone mapping spectrometer (TOMS) on Nimbus 7, with a field of view of 40 km square, do not support the existence of measurable localized depletion of ozone following a Space Shuttle launch.[8] (It should be noted that the TOMS data were taken at least 7 h after the Shuttle launch, and so any local ozone loss on a time scale less than that may not have been observed.)

In contrast to these arguments, measurements of local ozone loss greater than 40% below background was measured in the exhaust trail of a Titan III solid rocket at 13 min after launch.[9] Karol et al.[4] have calculated a local loss (within 1 km of the exhaust plume) of ozone to be greater than 80% between 1 and 3 h after launch.

This paper concentrates on modeling the local effects of launches by solid propellant engines that are smaller than the Shuttle. It is expected that the results will be qualitatively the same for the larger vehicles, and it should be possible to scale to the larger vehicles if desired. It will be shown that afterburning in the plume as it mixes with the atmosphere can cause significant chemical changes. For example, HCl is partially converted to more active chlorine species such as Cl before the plume reaches ambient temperature.

Stratospheric Chemistry of Rocket Effluents

The abundance of ozone in the stratosphere is controlled by a dynamic balance among chemical processes that produce or destroy it and physical processes that transport it to the

---

Received Sept. 25, 1992; revision received April 19, 1993; accepted for publication April 19, 1993.

*Currently president, Denison Development Inc. Member AIAA.

†Senior Scientist, Chemistry Technology Department.

‡Manager, Materials and Processes Department. Member AIAA.

§Staff Engineer, Fluid and Thermophysics Department.

¶Section Head, Fluid Thermophysics Department. Member AIAA.

troposphere. According to current understanding, two general classes of chemistry govern ozone abundance: homogeneous and heterogeneous. In terms of homogeneous chemistry, the most important photochemical reactions regulating ozone involve molecular and atomic oxygen and various radicals containing nitrogen, hydrogen, and chlorine.

Heterogeneous chemistry is a new and rapidly developing field and is very complex compared with homogeneous chemistry.[10–12] Heterogeneous chemistry involves those reactions that occur on surfaces in the stratosphere. It is now well recognized that heterogeneous processes are crucial to stratospheric chemistry in the polar regions and may play previously unsuspected roles in midlatitudinal regions as well. The particle chemistry has shown a tendency to enhance the destruction of stratospheric ozone, primarily through reactions involving chlorine, whose primary source is chlorofluorocarbons (CFCs).

The solid rocket motors in the hypothetical vehicle modeled in this study release about 9500 kg of chlorine into the stratosphere per launch. By far the dominant form of chlorine released is HCl. Afterburning reactions, as discussed later, can transform a significant fraction of the HCl into Cl_2 or Cl. Cl_2 photolyzes readily in the stratosphere, with a lifetime of several minutes, to form Cl radical. HCl itself does not react with ozone. The chlorine from HCl must be liberated by reaction with hydroxyl radical or, to a less extent, by solar photolysis.

One important mechanism for ozone destruction in the stratosphere occurs when a chlorine atom is produced. It can react with ozone to produce chlorine monoxide:

$$Cl + O_3 \rightarrow ClO + O_2 \tag{1}$$

One chlorine monoxide undergoes reaction with another chlorine monoxide:

$$ClO + ClO + M \rightarrow Cl_2O_2 + M \tag{2}$$

$$Cl_2O_2 + \text{sunlight} \rightarrow Cl + ClO_2 \tag{3}$$

$$ClO_2 + M \rightarrow Cl + O_2 + M \tag{4}$$

Reactions (1) through (4) result in a catalytic cycle in which ozone is destroyed and Cl is continuously regenerated. The principal sink for active chlorine species is conversion to hydrogen chloride.

The effect on stratospheric ozone of chlorine released by solid rocket motors is expected to be the same—on an atom-per-atom basis—as that of chlorine released by the decomposition of CFCs, if the altitude of injection is taken into account. The reason is that the various inorganic forms of chlorine rapidly interconvert to each other, whereas the altitude of injection merely determines the residence time in the stratosphere; the latitude of injection has an effect on the residence time, but it is not as pronounced as the altitude factor.

In addition to the homogeneous chlorine-induced catalytic processes, there is a potential for the aluminum oxide particles released from solid rocket motors to provide surfaces that promote chemical reactions releasing active chlorine. The TRW hypothetical vehicle releases about 20,000 kg of aluminum oxide into the stratosphere per launch. Using the scenario of nine Shuttle launches and six Titan launches per year established by Prather et al.,[3] Bennett et al.[13] estimated an increase in global aerosol surface from these particles to be on the order of 0.1%. The significance of this increase is not well established, and the chlorine activation by aluminum oxide is not currently well understood.

Hot Plume Chemistry

The chemistry of rocket exhaust is complex. To describe adequately the chemistry, one needs to start in the rocket combustion chamber and then work through the nozzle expansion process. After the gases have expanded through the nozzle, they mix and react with the atmosphere. To characterize the process and chemistry that occurs from the combustion chamber onward requires the use of numerical models.

Following Hoshizaki,[1] the rocket plume is divided into two parts: the hot plume and the cold plume. In the hot plume analysis, the rocket plume chemistry and the fluid dynamics are modeled from the combustion chamber, through the rocket nozzle, and out to the point where the plume temperature and pressure are equal to the ambient. Chemical equilibrium is assumed in the combustion chamber. However, as the flow expands into the nozzle, one-dimensional finite rate chemistry is adopted. In the cold plume regime, high-temperature homogeneous gas phase reactions become unimportant, and photochemically initiated reactions are of primary concern. In addition, species migration is dominated by the diffusion process in the cold plume regime.

A rigorous solution of the hot plume regime was adopted that involved basically three steps: 1) a chemical equilibrium calculation involving fuel and oxidizer, which determined the products in the combustion chamber; 2) a method of characteristic solution coupled with finite rate chemistry, which was used to characterize the flow and species in the nozzle; and 3) the finite difference method, which was used to determine the plume flowfield, including the intrinsic core and the mixing layer. Steps 1 and 2 were accomplished using the Solid Propellant Rocket Motor Performance Program (SPP).[14] This code calculates the gas phase flowfield as well as the particle phase. In all of the calculations, up to five particle groups were used. Step 3 was performed by the JANNAF Standardized Plume Flowfield Code (SPF-II).[15] The shock-capturing scheme employed in the SPF-II provides an inviscid, frozen chemistry solution to the plume near field. It accounts for the detailed shock structures and gas particle interactions. In an underexpanded plume the barrel shock may be strong enough to produce a Mach disk. The assumption of frozen chemistry appears to be invalid behind the Mach disk because the temperature behind it exceeds 2000 K. At this elevated temperature it is expected that a significant amount of NO_x will be generated. In SPF-II, the turbulent mixing component provides a viscous, turbulent solution of the plume shear layer with finite rate chemistry. With the inviscid flow conditions generated by the shock-capturing scheme as the inner boundary condition, the mixing layer component calculated the entire plume flowfield.

Table 1 shows the specifications for the TRW hypothetical solid rocket motor under consideration. Table 2 shows the chemical reactions used in the plume afterburning analysis. All reactions are reversible. Rate constants for the reverse reactions are calculated from the equilibrium constants. Many of the reactions were found to be unimportant in determining the species resulting from the nozzle and plume analysis but were included for completeness, especially in terms of evaluating their effect on HCl concentrations. Included in the kinetic mechanism were five detailed mechanisms describing the afterburning of hydrogen molecules, NO_x formation as given by the modified Zeldovich mechanism,[16] afterburning of carbon monoxide, dissociation

Table 1 Specifications of TRW hypothetical solid rocket motor

Propellant composition	Weight, %
Aluminum	19
Ammonium perchlorate	68.9
R-45/IPDI	10.7
DOA	1
HX-752	0.3
Fe_2O_3	0.1
Chamber pressure, psia	1275
Throat radius, in.	7
Nozzle exit ratio, in.	2.51
A/A*	18.5
Stratospheric chlorine release, kg	9,540
Stratospheric alumina release, kg	13,400

Table 2 Chemical reactions used to elucidate afterburning chemistry in SRM plume

	Reaction rate expression variables			
Reaction	*A*, $cm^3 molecule^{-1} s^{-1}$	*n*	*E*/*R*, K	Ref.
1 $O_2 + M \rightleftarrows O + O + M$	3.0×10^{-6}	−1	59,380	22
2 $HO_2 + NO \rightleftarrows NO_2 + OH$	3.7×10^{-12}	0	−240	17
3 $O + NO_2 \rightleftarrows NO + O_2$	6.5×10^{-12}	0	−120	23
4 $NO_2 + H \rightleftarrows NO + OH$	1.4×10^{-10}	0	0	23
5 $NO + O \rightleftarrows N + O_2$	3.5×10^{-15}	1	19,500	23
6 $O + N_2 \rightleftarrows NO + N$	1.3×10^{-10}	0	38,000	24
7 $NO + H \rightleftarrows N + OH$	2.8×10^{-10}	0	24,560	23
8 $N_2O + M \rightleftarrows N_2 + O + M$	1.2×10^{-6}	−0.73	31,600	23
9 $O + N_2O \rightleftarrows N_2 + O_2$	1.7×10^{-10}	0	14,100	23
10 $N + NO_2 \rightleftarrows N_2O + O$	3×10^{-12}	(298 K value)	——	25
11 $N_2O + H \rightleftarrows N_2 + OH$	1.6×10^{-10}	0	7,600	23
12 $NO_2 + H_2 \rightleftarrows HNO_2 + H$	3.98×10^{-11}	0	14,594	27
13 $HNO + H \rightleftarrows H_2 + NO$	3×10^{-11}	0	500	23
14 $HNO + OH \rightleftarrows H_2O + NO$	8×10^{-11}	0	500	23
15 $NO + M \rightleftarrows N + O + M$	2.4×10^{-9}	0	74,700	23
16 $N_2 + M \rightleftarrows N + N + M$	3.82×10^{5}	−3.5	113,240	24
17 $N + OH \rightleftarrows NO + H$	3.8×10^{-11}	0	−85	26
18 $Cl + O_3 \rightleftarrows ClO + O_2$	2.9×10^{-11}	0	260	17
19 $ClO + NO \rightleftarrows NO_2 + Cl$	6.4×10^{-12}	0	−290	17
20 $ClO + OH \rightleftarrows HO_2 + Cl$	1.1×10^{-11}	0	−120	17
21 $Cl + HO_2 \rightleftarrows HCl + O_2$	1.8×10^{-11}	0	−170	17
22 $Cl + HO_2 \rightleftarrows OH + ClO$	4.1×10^{-11}	0	450	17
23 $Cl_2 + OH \rightleftarrows HOCl + Cl$	1.4×10^{-12}	0	900	17
24 $HOCl + OH \rightleftarrows H_2O + ClO$	3×10^{-12}	0	500	17
25 $ClONO_2 + h\nu \rightleftarrows Cl + NO_3$	$5 \times 10^{-5} s^{-1}$	——	——	17
26 $H_2 + OH \rightleftarrows H_2O + H$	5.5×10^{-12}	0	2,000	17
27 $OH + O \rightleftarrows H + O_2$	2.2×10^{-11}	0	−120	17
28 $OH + H \rightleftarrows H_2 + O$	8.1×10^{-21}	2.8	1,950	22
29 $OH + OH \rightleftarrows H_2O + O$	4.2×10^{-12}	0	240	17
30 $OH + CO \rightleftarrows CO_2 + H$	7.29×10^{-18}	1.5	−373	26
31 $Cl + H_2 \rightleftarrows HCl + H$	3.7×10^{-11}	0	2,300	17
32 $OH + HCl \rightleftarrows Cl + H_2O$	2.6×10^{-12}	0	350	17
33 $Cl + H_2O \rightleftarrows HCl + OH$	2.79×10^{-11}	0	8,670	24
34 $HCl + O \rightleftarrows OH + Cl$	1×10^{-11}	0	3,300	17
35 $H + Cl_2 \rightleftarrows HCl + Cl$	1.43×10^{-10}	0	590	24

	Reaction rate expression variables			
Reaction	*A*, cm^6 $molecule^{-2} s^{-1}$	*n*	*E*/*R*, K	Ref.
36 $M + 2H \rightleftarrows H_2 + M$	1.5×10^{-29}	−1.3	0	22
37 $M + 2O \rightleftarrows O_2 + M$	5.21×10^{-35}	0	−900	22
38 $M + 2Cl \rightleftarrows Cl_2 + M$	6.14×10^{-34}	0	−906	24
39 $H + O + M \rightleftarrows OH + M$	1.3×10^{-29}	−1	−906	24
40 $H + OH + M \rightleftarrows H_2O + M$	6.11×10^{-26}	−2	0	22
41 $CO + O + M \rightleftarrows CO_2 + M$	1.7×10^{-33}	−2	0	22
42 $NO + O + M \rightleftarrows NO_2 + M$	4.7×10^{-26}	1.5	0	23
43 $OH + NO_2 + M \rightleftarrows HNO_3 + M$	1.77×10^{-15}	−5.49	1,187	22
44 $H + NO + M \rightleftarrows HNO + M$	2.47×10^{-28}	−1.32	370	23
45 $ClO + NO_2 + M \rightleftarrows ClONO_2 + M$	4.65×10^{-23}	−3.40	0	17
46 $OH + NO + M \rightleftarrows HNO_2 + M$	1.4×10^{-24}	−2.51	−34	23

of HCl, and finally the aluminum reaction mechanism. No sensitivity analysis was performed to determine the effect of each of the rate constants on the concentrations at the end of the hot plume region. However, the values are taken from the most recent compilation of rate constants used specifically for this purpose (see references to Table 3). In addition, classified work by several of the authors in the area of rocket engine and afterburning chemistry has shown that these equations and rate constants are, in general, sufficient.

Little NO_x was formed because, as the plume expands into the ambient atmosphere, the temperature drops well below 2000 K, where formation of NO_x is not favored. HO_x radicals are extremely important in afterburning, but their concentrations are typically very small, adding little to ozone depletion. HCl decomposes readily in the presence of atomic hydrogen. The reaction between Cl and H_2 to generate HCl (Reaction 31) is slow compared with the recombination of Cl in a third-body reaction (Reaction 38). Consequently a significant fraction of HCl was converted to Cl or Cl_2. Reactions in this region of the plume with the ambient atmosphere are of minor importance because the time for diffusion of the atmosphere into the plume is extremely short. A plot of the exhaust product concentration integrated across the plume as function of distance from the nozzle exit plane is shown in Fig. 1 for an altitude of 18 km and in Fig. 2 for an altitude of 30 km.

Cold Plume Dispersion and Reaction

Once the afterburning reactions are complete and the plume has essentially reached ambient temperature, the plume disperses into the surrounding atmosphere by diffusion and small-scale convective motions.

A plume dispersion model was developed by TRW to evaluate the chemical interaction of the plume with the ambient atmosphere. It is assumed that vertical transport within the stratosphere is small compared with horizontal transport. The

Table 3 Reactions for modeling plume dispersion chemistry for SRM

	Reaction rate expression variables			
Reaction	A, cm^{3}molecule^{-1}s^{-1}	*n*	*E*/*R*, K	Ref.
1 $S + HCl \rightarrow HCl.S$	a	——	——	——
2 $HCl.S + ClONO_2 \rightarrow Cl_2 + HNO_3.S$	a	——	——	——
3 $Cl_2 + hv \rightarrow Cl + Cl$	3×10^{-3}s^{-1}	0	0	28
4 $Cl + O_3 \rightarrow ClO + O_2$	2.9×10^{-11}	0	0	28
5 $ClO + O \rightarrow Cl + O_2$	3.0×10^{-11}	0	260	17
6 $ClO + HO_2 \rightarrow HOCl + O_2$	4.8×10^{-13}	0	−7	17
7 $OH + O_3 \rightarrow HO_2 + O_2$	1.6×10^{-12}	0	−700	17
8 $HOCl + hv \rightarrow OH + Cl$	5×10^{-4}s^{-1}	0	940	17
9 $NO + O_3 \rightarrow NO_2 + O_2$	2.0×10^{-12}	0	1400	17
10 $ClONO_2 + hv \rightarrow NO_3 + Cl$	5×10^{-5}s^{-1}	0	0	28
11 $NO_3 + hv \rightarrow NO + O_2$	2.0×10^{-2}	0	0	28
12 $Cl_2O_2 + M \rightarrow ClO + ClO + M$	1×10^{-3}s^{-1}	0	0	29
13 $Cl_2O_2 + hv \rightarrow 2Cl + O_2$	1×10^{-3}s^{-1}	0	0	29
14 $OH + CO \rightarrow CO_2 + H$	7.29×10^{-18}	1.5	−373	26
15 $ClO + NO \rightarrow Cl + NO_2$	6.4×10^{-2}	0	−290	17
	Reaction rate expression variables			
Reaction	A, cm^{6}molecule^{-2}s^{-1}	*n*	*E*/*R*, K	Ref.
16 $ClO + NO_2 + M \rightarrow ClONO_2 + M$	4.65×10^{-23}	−3.4	0	17
17 $ClO + ClO + M \rightarrow Cl_2O_2 + M$	1.45×10^{-23}	−3.6	0	17

[a] Reaction rate expression derived from collision theory. Probability is assumed to be similar to $ClONO_2$ on water ice, as explained in the text. S is some surface available for heterogeneous reaction.

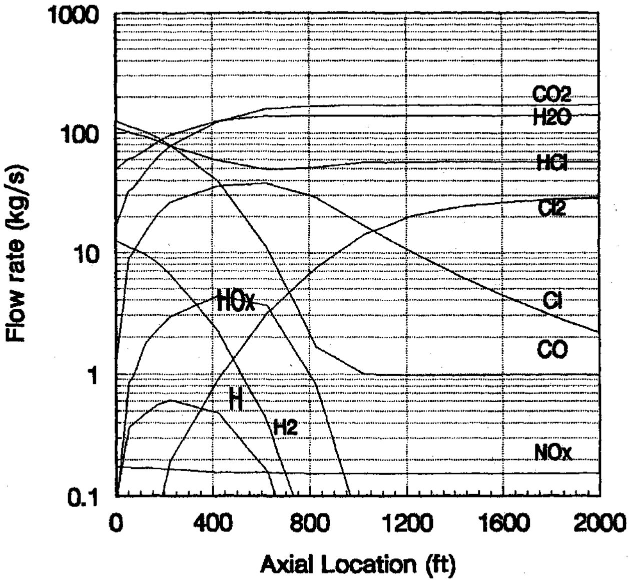

Fig. 1 Integrated species in hot plume region at 18 km.

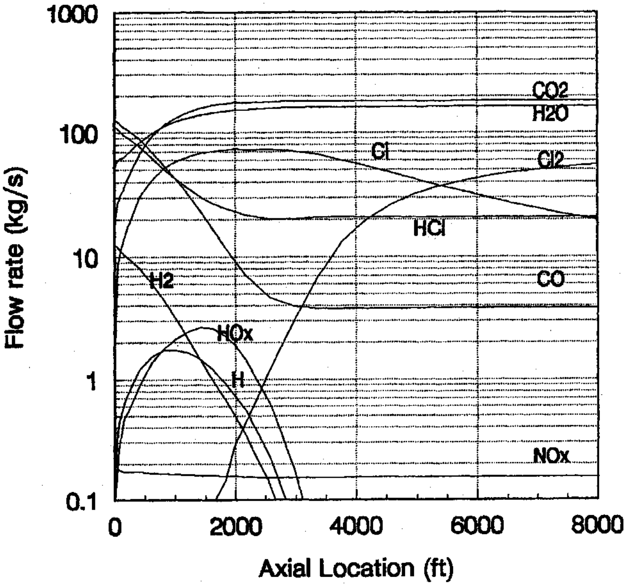

Fig. 2 Integrated species in hot plume region at 30 km.

plume is assumed to be a cylinder of gas that expands and reacts. As the plume expands, the concentrations of exhaust products relative to the background atmospheric concentrations change, and hence the chemical reactivity also changes. The plume dispersion model takes into account both transport and reaction in determining impact of exhaust on atmospheric constituents such as ozone.

It is assumed that in the early stages of plume dispersion the plume retains its identity and is not yet broken up by wind shears. The primary mechanism of dispersion after it comes to rest with respect to the local environment and its temperature reaches equilibrium is diffusion due to atmospheric turbulence. Advection is removed by allowing the origin of the coordinate system to move with the wind. The conservation equation for each species can be written

$$\frac{\partial N}{\partial t} = \frac{1}{r}\frac{\partial}{\partial r} rK \frac{\partial N}{\partial r} + \dot{R}_N \qquad (5)$$

For solid propellant rockets, a major constituent of the exhaust is solid aluminum oxide particles. There is a possibility that these particles may form sites for heterogeneous reactions similar to the role of ice crystals in clouds over Antarctica. In our calculations, the surface-to-volume ratio due to these particles in the exhaust is assumed to diffuse as a passive scaler. Since no direct measurements of heterogeneous reactions of chlorine compounds on aluminum oxide particles are available, the data of Leu and of Molina et al. (Described in DeMore et al.[17]) for ice crystals were used to estimate reaction probabilities for heterogeneous reactions on aluminum oxide. This represents a worst-case (fastest) scenario for heterogeneous chemistry on aluminum oxide. Clearly laboratory studies are essential to establishing a mechanism and rate for this reaction. Table 3 shows the chemical kinetic data used in modeling the plume chemistry.

Estimates of Turbulent Diffusivity

The magnitude of the turbulent diffusivity determines the residence time for chemical reactions. It turns out that differences in assumptions about turbulent diffusivity can have a large effect on the ozone depletion.

To estimate the effect of atmospheric turbulent diffusivity, it is tempting to use published values for the stratosphere. Warneck[18] gives a value of $K = 2 \times 10^6$ m^2 s^{-1}, whereas Williamson et al.[19] give $K = 2.5 \times 10^5$ m^2 s^{-1}.

An exact solution of Eq. (5) with no chemistry exists for the case of a cylinder of radius a containing an initial species density N_0 and zero density outside a (see Carslaw and Jaeger[20]). The solution on the centerline is

$$N = N_0\,[1 - \exp(-a^2/4Kt)] \qquad (6)$$

Using the value of K given by Warneck, for $a = 10$ m, it would take 1.2×10^{-4} s for the density on the centerline to decrease to 10%, whereas the Williamson value yields 9.5×10^{-4} s. These times are contrary to observations that plumes persist for many minutes.

An explanation for these contradictory results is that the plume is very small compared with the integral scale of atmospheric turbulence, which is on the order of tens of kilometers. Therefore, the apparent diffusivity of the plume should depend on the small eddies in the turbulent spectrum on the order of its own size.

An estimate of the apparent diffusivity as influenced by the appropriate scales can be obtained from statistical theory. From Taylor's theorem,

$$K = \overline{u'^2} \int_0^t R(\tau)\, \mathrm{d}\tau \qquad (7)$$

It is common to assume the form of the correlation function as

$$R(\tau) = \exp(-\tau/t_L) \qquad (8)$$

Then

$$K = \overline{u'^2}\, t_L \left[1 - \exp\left(-t/t_L\right)\right] \qquad (9)$$

For large t/t_L,

$$K = \overline{u'^2}\, t_L \qquad (10)$$

where $t_L = 4.2 \times 10^4$ s (see Möller[21]). If u' is about 7 m s^{-1}, $K = 2 \times 10^6$ m^2 s^{-1}, which is the value of Warneck.

For small t/t_L,

$$K = \overline{u'^2}\, t \qquad (11)$$

One can estimate $t = l/u'$. If the scale l is about 10 m, $K = 70$ m^2 s^{-1}. This smaller value for the eddy diffusivity should lead to more reasonable residence times.

Although there is no comprehensive database of plumes in the stratosphere, some measurements have been reported. For example, Hoshizaki[1] has presented optical measurements of the exhaust plume of a large solid booster at 60,000 ft. It was pointed out that such measurements should be strongly dependent on atmospheric conditions. Nevertheless, it is instructive to attempt to deduce an apparent diffusivity from the data.

It can be shown that if the diffusivity is constant, a solution to Eq. (5) for a line source is

$$N = A \exp(-r^2/4Kt)/t \qquad (12)$$

The method of detecting the edge of the plume had to be instrument dependent with some subjective judgment of the operator. Whatever the criterion, it probably depended on some approximately constant level of number density N. Therefore, if Eq. (12) describes the phenomenon, a plot of the Hoshizaki data in the form $r^2/4t$ vs $\ln(t)$ should be a straight line with a negative slope equal to K. The data are plotted in this manner in Fig. 3. No discernable trend can be seen.

If, as suspected, the diffusion depends on the size of the plume, an alternate solution for a line source [Eq. (5)] can be obtained:

$$N = B \exp(-r/bt)/t^2 \qquad (13)$$

where $K = br$. If Eq. (13) holds, a plot of r/t vs $\ln(t)$ should be a straight line with a negative slope of $2b$. It can be seen in Fig. 4 that this method of plotting the data brings order out of chaos. The average value of the slope is about 2.2. For a 10-m plume radius, this would yield a value of 11 m^2 s^{-1} or a factor of six lower than that deduced from statistical theory. Considering all of the uncertainties in both approaches to estimating apparent diffusivity, the agreement is remarkable.

Numerical Methods

A special code was written for the local dispersion with finite rate chemistry. An implicit method of computation was used

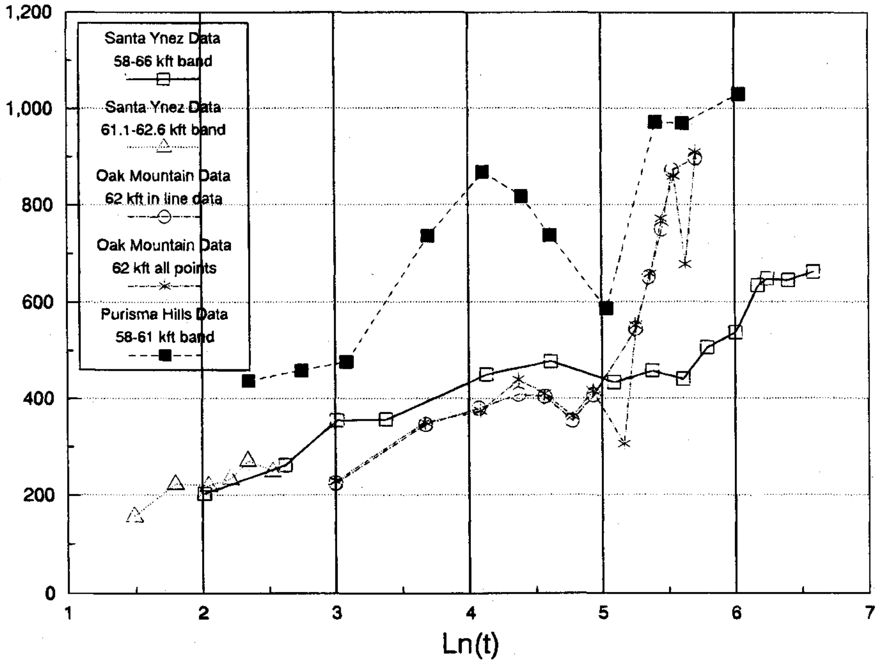

Fig. 3 Eddy diffusion fit to rocket plume growth data assuming constant diffusivity [$N = A \exp(-r^2/4kt)/t$].

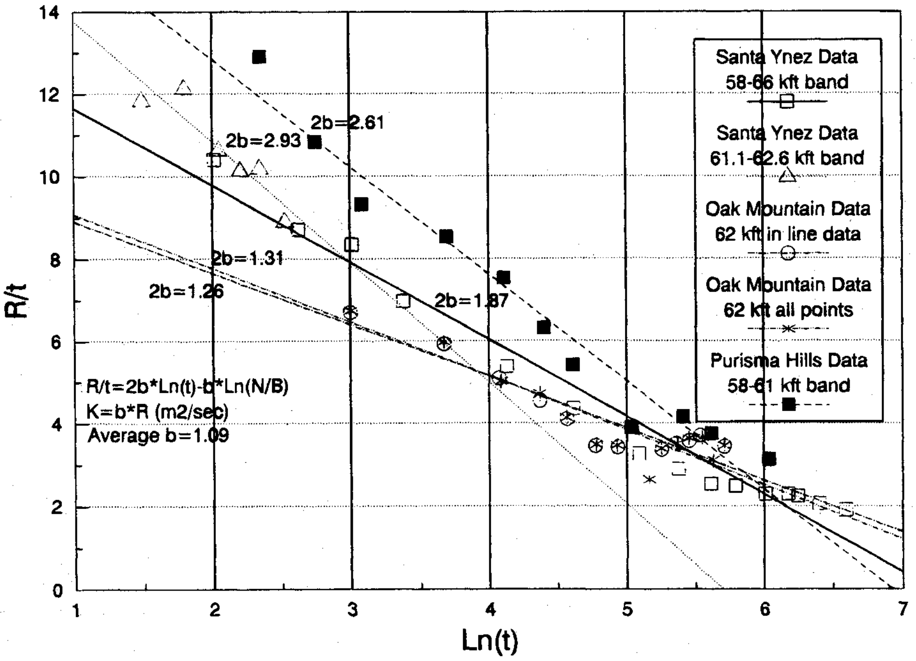

Fig. 4 **Eddy diffusion fit to rocket plume growth data assuming variable diffusivity [$N = B \exp(-r/bt)/t^2$].**

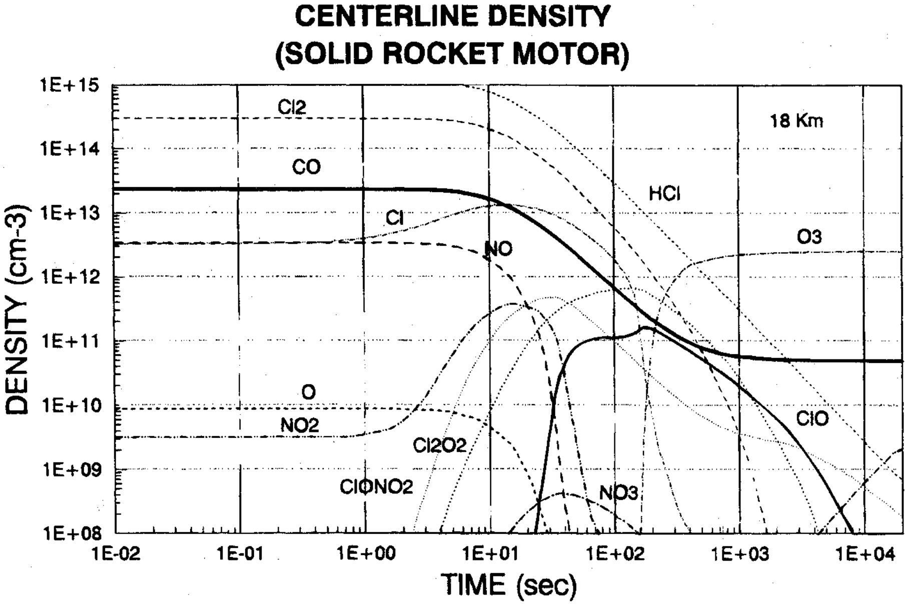

Fig. 5 **Cold plume diffusion and chemistry at 18 km.**

with unequal grid spacing to resolve regions of strong gradients. By taking account of the diagonalized form of the matrix of coefficients, the entire field is solved at each time step by Gaussian elimination. The average running time on Silicon Graphics 4D/240 IRIS workstation is about 10 min.

Results

The species density on the centerline of the plume is shown as a function of time for the TRW hypothetical solid rocket at 18 and 30 km in Figs. 5 and 6. It can be seen that at both altitudes the initial conditions produced a large amount of Cl_2 and Cl as a result of afterburning. The result is that the ozone that was displaced by the initial plume does not immediately diffuse back to the centerline. Instead, some depletion of ozone takes place near the edge of the plume until the chlorine concentration is reduced by diffusion to a level such that the excess ozone can diffuse into the core of the plume. This begins to occur at about 65 s at 18 km and 120 s at 30 km. Soon thereafter the ozone reaches the ambient level at the core of the plume.

Some numerical experiments were run to test the impact of Cl and Cl_2. When both were arbitrarily removed, but HCl was retained in its original concentration, little ozone destruction occurred. This illustrates that for local ozone depletion the other homogeneous reactions listed in Table 3 as well as the heterogeneous reactions with Al_2O_3 particles were ineffective in local destruction of ozone.

The ozone depletion is illustrated in Figs. 7 and 8 at the same two altitudes as Figs. 5 and 6. To estimate depletion, ozone number density was calculated by allowing ozone to diffuse back into the plume both with and without chemical reactions. The depletion was estimated by taking the ratio ofthe chemically active ozone to inactive ozone averaged over finite radii at a particular time. The results were averaged over cylinders whose radii ranged from about 10 to 9600 m. By defining

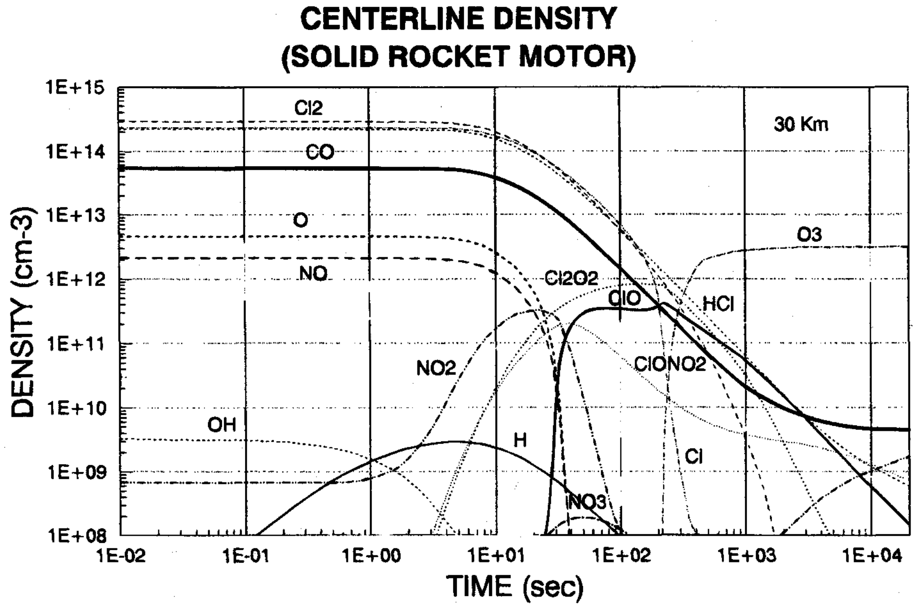

Fig. 6 Cold plume diffusion and chemistry at 30 km.

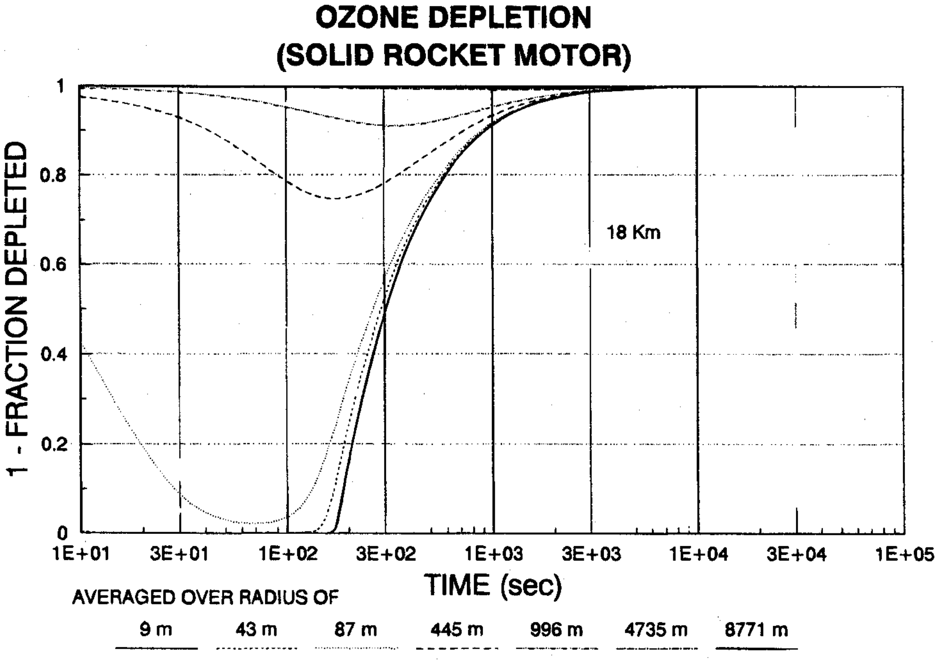

Fig. 7 Ozone depletion by chemical reaction at 18 km.

depletion in this manner, the reduction of ozone by displacement alone is eliminated as measure of depletion.

Conclusions

Comparison of the results presented here with those of Karol et al.[4] show that, although both models predict an effect on ozone in the locality of the rocket plume, the duration of the effect is very different. Our results show ozone loss for several minutes, whereas Karol et al. show the loss continuing for several hours. The details of their modeling scheme are not apparent. However, two points are clear: the details of their Scheme for taking into account afterburning chemistry are not apparent, and their initial diffusion constants for the cold plume were smaller than the ones used in this study. Any lack of afterburning chemistry in their model means that they should show less ozone destruction than our model. However, it is clear that the amount of ozone depletion is intimately tied to the value for the diffusion constant. With less diffusion, there is less break up of the plume and a longer time for the ozone-depleting reactions to occur. It is unlikely that the difference in ozone depletion can be due to the larger vehicles considered by Karol et al.

In our work we have developed a model beginning in the rocket combustion chamber that culminates in the effects of the rocket exhaust and afterburning species on stratospheric ozone. The calculated depletion is a strong function of the diffusion coefficient. Our diffusion coefficient was determined from a single set of observational data. Any heterogeneous chemistry that may have been occurring was far less important than the homogeneous chemistry on this time scale for the local plume. Our calculations are consistent with a local ozone depletion over a very short time period of a few minutes.

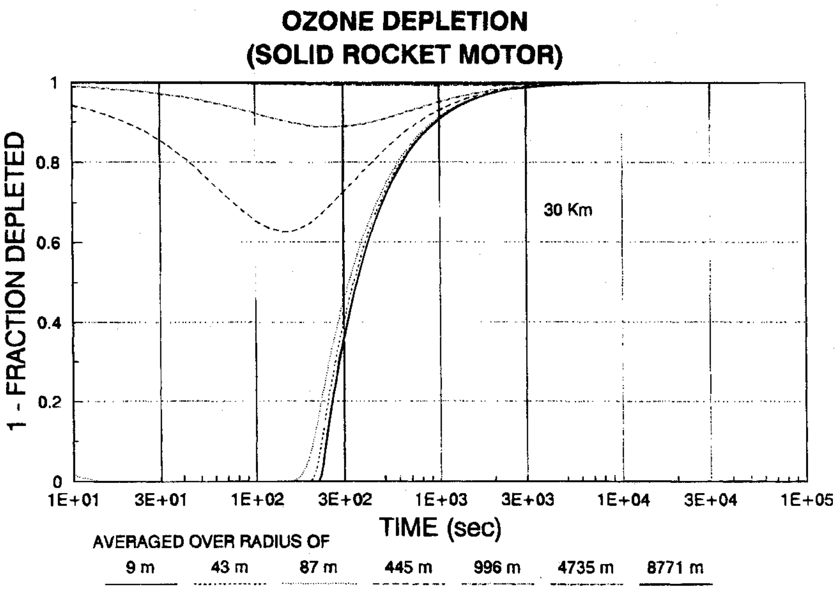

Fig. 8 Ozone depletion by chemical reaction at 30 km.

References

[1] Hoshizaki, H., "Aircraft Wake Microscale Phenomena," *The Stratosphere Perturbed by Propulsion Effluents,* Climatic Impact Assessment Program, U.S. Dept. of Transportation, CIAP Monogr. 3, Washington, DC, Sept. 1975, Chap. 2, pp. 60–73.

[2] Prather, M. J., Garcia, M. M., Douglass, A. R., Jackman, C. H., Ko, M. K. W., and Sze, N. D., "An Assessment of the Impact on Stratospheric Chemistry and Ozone Caused by the Launch of the Space Shuttle and Titan IV," *Present State of Knowledge of the Upper Atmosphere 1990: An Assessment Report,* NASA Reference Publication 1242, 1990, pp. 111–122.

[3] Prather, M. J., Garcia, M. M., Douglass, A. R., Jackman, C. H., Ko, M. K. W., and Sze, N. D., "The Space Shuttle's Impact on the Stratosphere," *Journal of Geophysical Research,* Vol. 95, No. D11, 1990, pp. 18,583–18,590.

[4] Karol, I. L., Ozolin, Y. E., and Rozanov, E. V., "Effect of Space Rocket Launches on Ozone and Other Atmospheric Gases," European Geophysical Association Conference, Wiesbaden, Germany, 1991.

[5] Pyle, J. A., and Jones, A. E., "An Investigation of the Impact of the Ariane-5 Launches on Stratospheric Ozone," European Space Agency, 1991.

[6] Anon., "Atmospheric Effect of Chemical Rocket Propulsion," AIAA Workshop Report, AIAA, Washington, DC, Oct. 1991.

[7] Turco, R. P., Toon, O. B., Whitten, R. C., and Cicerone, R. J., "Space Shuttle Ice Nuclei," *Nature,* Vol. 298, No. 5877, Aug. 1982, pp. 830–832.

[8] McPeters, R., Prather, M., and Doiron, S., "Reply to 'Comment on "The Space Shuttle's Impact on the Stratosphere," ' " *Journal of Geophysical Research,* Vol. 96, No. D9, 1991, pp. 17,379–17,381.

[9] Stewart, R. B., and Gomberg, R. I., "The Production of Nitric Oxide in the Troposphere as a Result of Solid-Rocket-Motor Afterburning," NASA TN D-8137, March 1976.

[10] Solomon, S., "Progress Towards a Quantitative Understanding of Antarctic Ozone Depletion," *Nature,* Vol. 347, No. 6291, Sept. 1990, pp. 347–354.

[11] Molina, M. J., "Heterogeneous Chemistry on Polar Stratospheric Clouds," *Atmospheric Environment,* Vol. 25A, Feb. 1991, pp. 2335–2345.

[12] Anon., "Scientific Assessment of Ozone Depletion: 1991," World Meteorological Organization, Global Ozone Research and Monitoring Project, Rept. 25, Geneva, Switzerland, 1992.

[13] Bennett, R. R., Hinshaw, J. C., and Barnes, M. W., "The Effects of Chemical Propulsion on the Environment," International Astronautical Federation Conference, Montreal, Quebec, Canada, Oct. 1991; see also *Acta Astronautica,* Vol. 26, No. 7, 1992, pp. 531–541.

[14] Nickerson, G., Kulick, F., and Dang, A., "The Solid Propellant Rocket Motor Performance Program, Version 6.0," Software and Engineering Associates, Inc. Carson City, NV, AFA1-TR-87-078, Dec. 1987.

[15] Dash, S., Pergament, H., Wolf, D., Sinha, N., Taylor, M., and Vaughn, M., Jr., "JANNAF Standardized Plume Flowfield Code, Version II," U.S. Army Missile Command, TR CR-RD-5S-90-4, Redstone, AL, July 1990.

[16] Zeldovich, Y., *Acta Physecochem USSR,* Vol. 21, 1946, p. 577.

[17] DeMore, W. B., Sander, S. P., Golden, D. M., Molina, M. J., Hampson, R. F., Kurylo, M. J., Howard, C. J., and Ravishankara, A. R., "Chemical Kinetics and Photochemical Data for Use in Stratospheric Modeling," NASA Panel Data Evaluation, Jet Propulsion Lab., California Inst. of Technology, JPL Publication 90-1, Pasadena, CA, Jan. 1990.

[18] Warneck, P., *The Chemistry of the Natural Atmosphere,* Academic Press, San Diego, CA, 1988, p. 20.

[19] Williamson, D. L., Kiehl, J. T., Ramanathan, V., Dickinson, R. E., and Hack, J. J., "Description of NCAR Community Climate Model (CCMI)," NCAR, NCAR/Tn-285 + STR, Boulder, CO, June 1987, p. 30.

[20] Carslaw, H. S., and Jaeger, J. C., *Conduction of Heat in Solids,* Oxford at the Clarendon Press, London, England, 2nd ed., 1959, p. 260.

[21] Möller, F., "Eine Berechnung des Horizontalen Grossaustausches über dem Atlantischen Ozean," *Arch. Meterol. Geophys. Bioklimatol.,* Ser. A2, pp. 73–81.

[22] Tsang, W., and Hampson, R. F., "Chemical Kinetic Data Base for Combustion Chemistry, Part I: Methane and Related Compounds," *Journal of Physical Chemical Reference Data,* Vol. 15, No. 3, 1986, pp. 1087–1280.

[23] Tsang, W., and Herron, J. T., "Chemical Kinetic Data Base for Propellant Combustion, I: Reactions Involving NO, NO_2; HNO, HNO_2, HCN and N_2O," *Journal of Physical Chemical Reference Data,* Vol. 20, No. 4, 1991, pp. 609–663.

[24] Kewley, D. J., and Hornung, H. G., "Free-Piston Shock-Tube Study of Nitrogen Dissociation," *Chemical Physics Letters,* Vol. 25, 1974, p. 531.

[25] Hanson, R. K., and Salimian, S., "Survey of Rate Constants in N/H/O System," *Combustion Chemistry,* edited by W. C. Gardiner Jr., Springer-Verlag, New York, 1984.

[26] Atkinson, R., Baulch, D. L., Cox, R. A., Hampson, R. F., Jr., Kerr, J. A., and Troe, J., "Evaluated Kinetic and Photochemical Data for Atmospheric Chemistry: Supplement III," *Journal of Physical Chemical Reference Data,* Vol. 18, No. 2, 1989, p. 881.

[27] Slack, M. W., and Grillo, A. R., "Rate Coefficients for $H_2 + NO_2 = HNO_2 + H$ Derived from Shock Tube Investigation of the H_2-O_2-NO_2 Ignition," *Combustion and Flame,* Vol. 31, 1978, p. 275.

[28] Brasseur, G., and Solomon, S., *Aeronomy of the Middle Atmosphere,* 2nd ed., D. Reidel Publishing Co., Norwell, MA, 1986.

[29] Anon., "Scientific Assessment of Stratospheric Ozone: 1989," World Meteorological Organization, Global Ozone Research and Monitoring Project, Rept. 20, Geneva, Switzerland.

James A. Martin
Associate Editor